ARTICLE

Oral Curcumin Mitigates the Clinical and Neuropathologic Phenotype of the *Trembler-J* Mouse: A Potential Therapy for Inherited Neuropathy

Mehrdad Khajavi, Kensuke Shiga, Wojciech Wiszniewski, Feng He, Chad A. Shaw, Jiong Yan, Theodore G. Wensel, G. Jackson Snipes, and James R. Lupski

Mutations in myelin genes cause inherited peripheral neuropathies that range in severity from adult-onset Charcot-Marie-Tooth disease type 1 to childhood-onset Dejerine-Sottas neuropathy and congenital hypomyelinating neuropathy. Many myelin gene mutants that cause severe disease, such as those in the myelin protein zero gene (*MPZ*) and the peripheral myelin protein 22 gene (*PMP22*), appear to make aberrant proteins that accumulate primarily within the endoplasmic reticulum (ER), resulting in Schwann cell death by apoptosis and, subsequently, peripheral neuropathy. We previously showed that curcumin supplementation could abrogate ER retention and aggregation-induced apoptosis associated with neuropathy-causing *MPZ* mutants. We now show reduced apoptosis after curcumin treatment of cells in tissue culture that express *PMP22* mutants. Furthermore, we demonstrate that oral administration of curcumin partially mitigates the severe neuropathy phenotype of the *Trembler-J* mouse model in a dose-dependent manner. Administration of curcumin significantly decreases the percentage of apoptotic Schwann cells and results in increased number and size of myelinated axons in sciatic nerves, leading to improved motor performance. Our findings indicate that curcumin treatment is sufficient to relieve the toxic effect of mutant aggregation-induced apoptosis and improves the neuropathologic phenotype in an animal model of human neuropathy, suggesting a potential therapeutic role in selected forms of inherited peripheral neuropathies.

Human inherited peripheral neuropathies are often a manifestation of peripheral myelin dysfunction and have long been proposed to result from abnormalities in Schwann cells and their myelin sheath and perturbed axon-glia interactions. The hereditary motor and sensory neuropathies are the largest class of hereditary neuropathies and include Charcot-Marie-Tooth disease (CMT) types 1 and 2 (CMT1 [MIM 118200] and CMT2 [MIM 600882]), hereditary neuropathy with liability to pressure palsies (HNPP [MIM 162500]), Dejerine-Sottas neuropathy (DSN [MIM 145900]), and congenital hypomyelinating neuropathy (CHN [MIM 605253]). CMT is the most common inherited disorder of the peripheral nervous system, with an estimated frequency of 1 in 2,500 individuals.[1] Patients with CMT usually manifest symptoms in the 1st or 2nd decade, with slowly progressive, symmetrical, length-dependent neuropathy leading to weakness of the distal muscles of the legs and feet, followed in most cases by involvement of the hands.[2–4] CMT1, the demyelinating form, is characterized by a slowing of the motor-nerve conduction velocities (usually to <38 m/s).[2]

The molecular cause of CMT1 in the majority of patients is a duplication of a 1.4-Mb region on the short arm of chromosome 17, to which the dosage-sensitive peripheral myelin protein 22 gene (*PMP22*) maps.[5–7] The reciprocal deletion of the same region is associated with a milder disease, HNPP.[8–10] PMP22, a 22-kDa glycoprotein with four putative transmembrane domains, comprises 2%–5% of peripheral nervous system myelin[11] and is found uniformly in compact regions of myelin.[12,13] Although PMP22 is widely expressed, by far the largest amount of PMP22 is produced by myelinating Schwann cells. It is clear from both human studies[7] and animal models[14] that alteration in *PMP22* gene dosage and expression has profound effects on the development and maintenance of peripheral nerves.[2,10] Consequently, the regulation of *PMP22* gene expression has been the focus of therapeutic strategies for CMT1A.[15–16] Onapristone, a progesterone antagonist, slows the disease progression by reducing the level of overexpression of *PMP22* in a CMT1A transgenic rat model, consequently improving the CMT phenotype.[15] Ascorbic acid treatment also significantly improves locomotor performance of CMT1A transgenic mouse models, possibly by blunting stimulation of cyclic adenosine monophosphate and thereby reducing the expression of *PMP22* to below the threshold level, enough to partially ameliorate the neuropathy.[16] These therapeutic approaches show promise in animal studies, but they are not feasible for other genetic causes of CMT because such molecular strategies apply only to *PMP22* overexpression.

PMP22 point mutations can also cause demyelinating neuropathies, such as CMT1, DSN, CHN, and HNPP (In-

herited Peripheral Neuropathies Mutation Database). The spontaneously occurring mouse models for CMT1, *Trembler-J* (*Tr-J*) (with mutation L16P) and *Trembler* (*Tr*) (with mutation G150D) result from dominantly transmitted *PMP22* missense mutations.[17,18] More recently, additional mouse *Pmp22* mutations that phenocopy more-severe human peripheral neuropathies, such as DSN, were isolated in a large-scale ethylnitrosourea mutagenesis screen.[19] Of note, severely affected patients with CMT1 with identical mutations and nerve biopsy results showing alterations analogous to those detected in heterozygous *Tr-J* and *Tr* mice have been described.[14,20,21] The pathomechanism for how these mutations affect myelination remains unknown; however, recent studies have shown that post-translational events, such as protein processing, trafficking, and accumulation in different intracellular compartments, are critical for myelination of Schwann cells.[22–25]

Recent experiments in diverse disease animal models suggest that curcumin enables misfolded proteins to traverse from the endoplasmic reticulum (ER) to the plasma membrane,[26–29] concurrently reducing the cytotoxicity of the mutant protein. Such observations have led us to explore the effects of curcumin in wild-type *PMP22, Tr-J,* and *Tr* mutants, using both cell-based and whole-animal assays. We studied the effects of curcumin on the wild-type and aggregation-induced apoptosis associated with disease-causing mutant PMP22 in transiently transfected HeLa cells. As we had observed previously for disease-associated *MPZ* alleles,[29] the Tr-J and Tr mutant proteins appear to be partially released from the ER after curcumin treatment; this is also associated with reduced apoptosis of cells in tissue culture. To evaluate the effects of curcumin in vivo, curcumin was administered orally to *Tr-J* mice. We observed considerable improvement of the neuropathy, including both the motor performance and the histopathology of the treated *Tr-J* mice, suggesting a potential therapeutic use for curcumin in severe forms of inherited peripheral neuropathy.

Material and Methods
Recombinant Constructs

Full-length human *PMP22* cDNA was subcloned into expression vector pcDNA3.1 (Invitrogen). Mutations were generated in each construct by use of the QuikChange site-directed mutagenesis kit (Stratagene). Primer sets were designed to create the following mutations: 47T→C (L16P; *Tr-J*) and 449G→C (G150D; *Tr*). Clones were verified by direct double-stranded DNA sequencing with use of the DyePrimer chemistry and ABI 377 sequencer (Applied Biosystems).

Tissue Culture, Transfection, and Immunostaining

HeLa cells were grown on a 6-well chamber flask and 4-well slides in Dulbecco's modified Eagle medium (BioWhittaker), supplemented with 10% fetal bovine serum, and were transfected with use of Lipofectamine 2000 (Invitrogen) in accordance with the supplier's instructions. Cells were incubated for 24 h at 37°C in a humidified incubator containing 10% CO_2. Cells were fixed

with 2% paraformaldehyde in PBS at room temperature for 10 min. The fixed cells were then washed and permeabilized with 0.1% Triton-X 100 in PBS on ice for 2 min. The cells were rinsed twice with PBS and were blocked with 5% normal goat serum in PBS for 1 h at 37°C. They were incubated with primary antibodies diluted in PBS with 1% normal goat serum at appropriate concentrations for 1 h at 37°C. The primary antibodies used in this study included the rabbit polyclonal antibody against PMP22 protein (1:1,000 [Novus Biologicals]) and the mouse monoclonal protein disulfide isomerase (PDI) (1:2,000 [Affinity Bioreagents]). This incubation was followed by two washes in PBS and incubation with Alexa Fluor goat anti-rabbit antibody (1:1,000 [Invitrogen Molecular Probe]) for 1 h at 37°C. For visualization of the nuclei, SlowFade Antifade Kit with 4′6-diamino-2-phenylindole (DAPI) (Invitrogen Molecular Probe) was used in accordance with the manufacturer's instructions. Fluorescently labeled cells were visualized by standard fluorescent microscopy.

Apoptosis Assay and Flow-Cytometric Analysis

Terminal deoxynucleotidyl transferase biotin-dUTP nick end labeling (TUNEL) staining was performed with use of an in situ cell-death detection kit, Fluorescein (Roche Applied Science). Cells were grown in four chamber slides and were fixed with 4% paraformaldehyde in PBS at room temperature for 10 min. Cells were then washed and permeabilized with 0.1% Triton-X 100 in PBS on ice for 2 min. TUNEL staining was performed in accordance with the conditions recommended by the supplier (for 1 h at 37°C). The average numbers of TUNEL-positive and DAPI-positive cells were calculated in 10 different sections, and the SD of the ratio was determined for each slide. Student's *t* tests comparing wild-type PMP22 and its mutants were performed. Statistical significance was defined by $P < .05$. For fluorescence-activated cell sorting (FACS) analysis, cells were transiently transfected for 24 h and then were harvested. Staining with annexin V, fluorescein isothiocyanate (FITC), and propidium iodide (BD Biosciences Pharmingen) was performed by the incubation of cells (1×10^6 cells/ml) in the dark for 25 min at room temperature in a binding buffer (10 mM HEPES, 140 mM NaCl, and 2.5 mM $CaCl_2$, at pH 7.4) containing a saturating concentration of annexin V, FITC, and propidium iodide. After incubation, the cells were washed, pelleted, and analyzed in an FACScan analyzer (Becton Dickinson). For in vivo TUNEL analysis, sciatic nerves were removed from mice immediately after death and were cut and fixed in 2.5% gluteraldehyde and 0.5% paraformaldehyde in 0.1 M phosphate buffer for at least 2 h. Nerve segments were then dehydrated in a graded series of ethanol and were embedded in paraffin. Longitudinal sections, 7 μm thick, were mounted on slides and then were dewaxed and rehydrated. In vivo TUNEL analysis was performed using ApopTag Peroxidase *In Situ* Apoptosis Detection kit (Chemicon International) in accordance with the supplier's instructions.

Genotyping

Genomic DNA was isolated from the tails of newborn mouse pups, and *Tr-J* mice (C57BL/6J) were genotyped as described elsewhere.[22]

Curcumin Treatment

Curcumin was purchased from Sigma (catalog number C7727). For cell culture treatment, curcumin stock was dissolved in di-
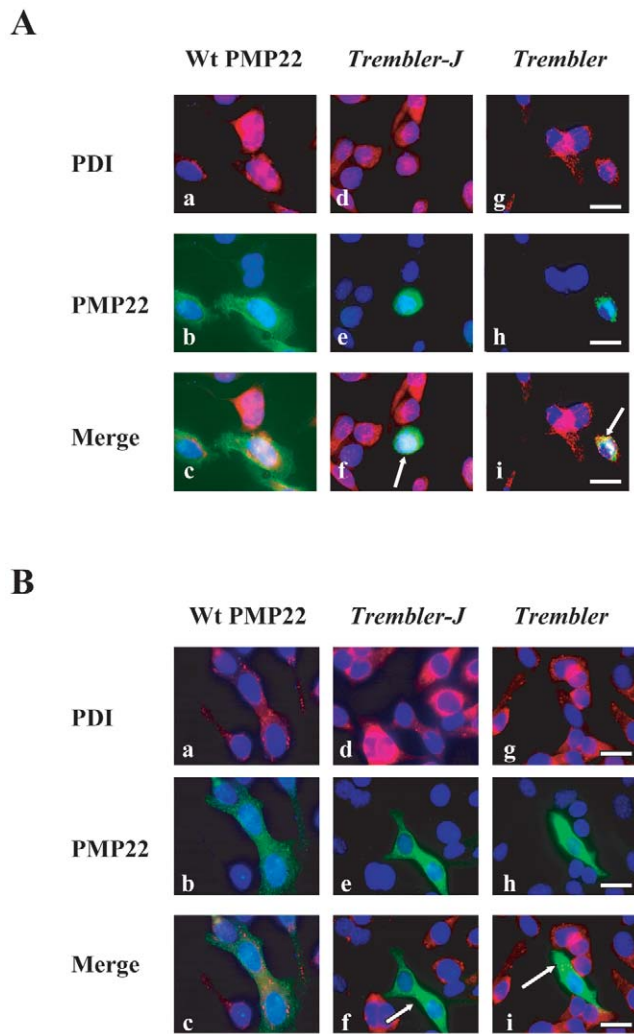
A

B

Figure 1. Release of ER-retained Tr-J and Tr mutants with curcumin treatment. *A,* Subcellular localization of wild-type (Wt) PMP22, Tr-J, and Tr in transiently transfected HeLa cells. Tr-J and Tr are extensively retained in the ER, as evidenced by colocalization with PDI (*arrows* in *f* and *i*). *B,* Curcumin treatment of HeLa cells rescues Tr-J and Tr mutants (*green*) retained in the ER (PDI markers [*red*]), as revealed by increased cytoplasmic staining. Cells treated with 40 μM curcumin showed reduced ER retention (*arrows* in *f* and *i*). Scale bars = 25 μm.

methylsulfoxide in accordance with the conditions recommended by the supplier. Cells were pretreated with curcumin (40 μM) for 3 h before transfection. For mice treatment, curcumin stock was dissolved in alimentum for 1 h before treatment. Each animal was treated with a daily dose of 0, 50, or 100 mg of curcumin per kg of body weight by gastric lavage for 90 d.

Rotarod Analysis

Groups of treated and nontreated littermates were placed on a round bar that was rotating initially at 16 rpm. The rotation speed was increased every minute from 16 to 36 rpm in steps of 4 rpm. The holding time of animals on the rotating rod was measured, and they were allowed to stay on the rod for a maximum of 270 s. Each animal was tested in two sessions of three trials each per day for 3 consecutive days.

Curcumin Bioavailability Assay

Two different age groups of mice (2-wk-old and 3-mo-old *Tr-J* mice) were treated with 100 mg of curcumin per kg of body weight by gastric lavage. At 0, 30, or 120 min after curcumin administration, animals were euthanized with isoflurane. Blood was collected by heart puncture and was mixed with EDTA (pH 8.0). Brain, liver, and sciatic nerve tissues were removed and homogenized with 0.1 M KH_2PO_4 (pH 3.0) and then were extracted twice with ethylacetate:isopropanol (9:1 v/v). The organic phase was dried under argon and then was resolved with 50% acetonitrile containing 0.1% trifluoroacetic acid (TFA). The samples were injected into a C18 column, and the curcumin was eluted with an acetonitrile gradient from 30% to 100%. Because of the low amount of curcumin in the small volume of sciatic nerve, curcumin was not detectable in sciatic nerves by a UV/visible (UV/VIS) detector. We used fluorescence detectors for curcumin detection in sciatic nerves. For mass spectrometry, mass spectral analysis was performed on a Finnigan LCQ DecaXP-plus quadrupole ion-trap mass spectrometer (ThermoFinnigan). The curcumin standard (Sigma) and elution fractions from high-performance liquid chromatography (HPLC) of mouse tissue extracts were dissolved in 50% acetonitrile (v/v) containing 0.1% TFA. The sample was loaded in an EconoTip (NewObjective), which was mounted on the nanospray electrospray ionization tip adaptor. Samples were analyzed in positive ionization mode over the range 150–1,000 m/z. The ion spray voltage was set at 2.0 kV, capillary temperature was 250°C, capillary voltage was 20 V, tube lens offset was -5 V, ion gauge pressure was 1.2×10^{-5} Torr, activation Q-value was 0.25, normalized collision energy was 35%, and the tandem mass spectrometry (MS/MS) isolation width was 1.0 m/z. The curcumin $[M+H]^+$ ion at 368.2 m/z was selected as the parent ion for the MS/MS scan. The fragmentation pattern of each elution fraction in the MS/MS analysis was manually compared with that of the curcumin standard.

Electron Microscopy

Sciatic nerves were harvested from mice euthanized with isoflurane. The nerves were immersion fixed in 2.5% gluteraldehyde and 0.5% paraformaldehyde in 0.1 M phosphate buffer for at least 2 h and were postfixed in 1% osmium tetroxide before being embedded in Spurrs resin. For light microscopy, 1-μm sections were stained with paraphenylenediamine and were observed by phase-contrast optics on a Zeiss Axioskop 2. For electron microscopy, thin sections were counterstained with lead citrate and uranyl acetate. For statistical analysis, we performed a one-way analysis of variance (ANOVA) on the normalized data. The F statistic for this ANOVA was $F = 2,459.3$, for an F statistic on 3 and 3,213 df.

Results
Curcumin's Reversal of Induction of Apoptosis

Previous studies have shown that *PMP22* is associated with ER chaperones during normal folding and that such interactions are more prolonged with PMP22 mutants during quality control, causing retention in the ER of
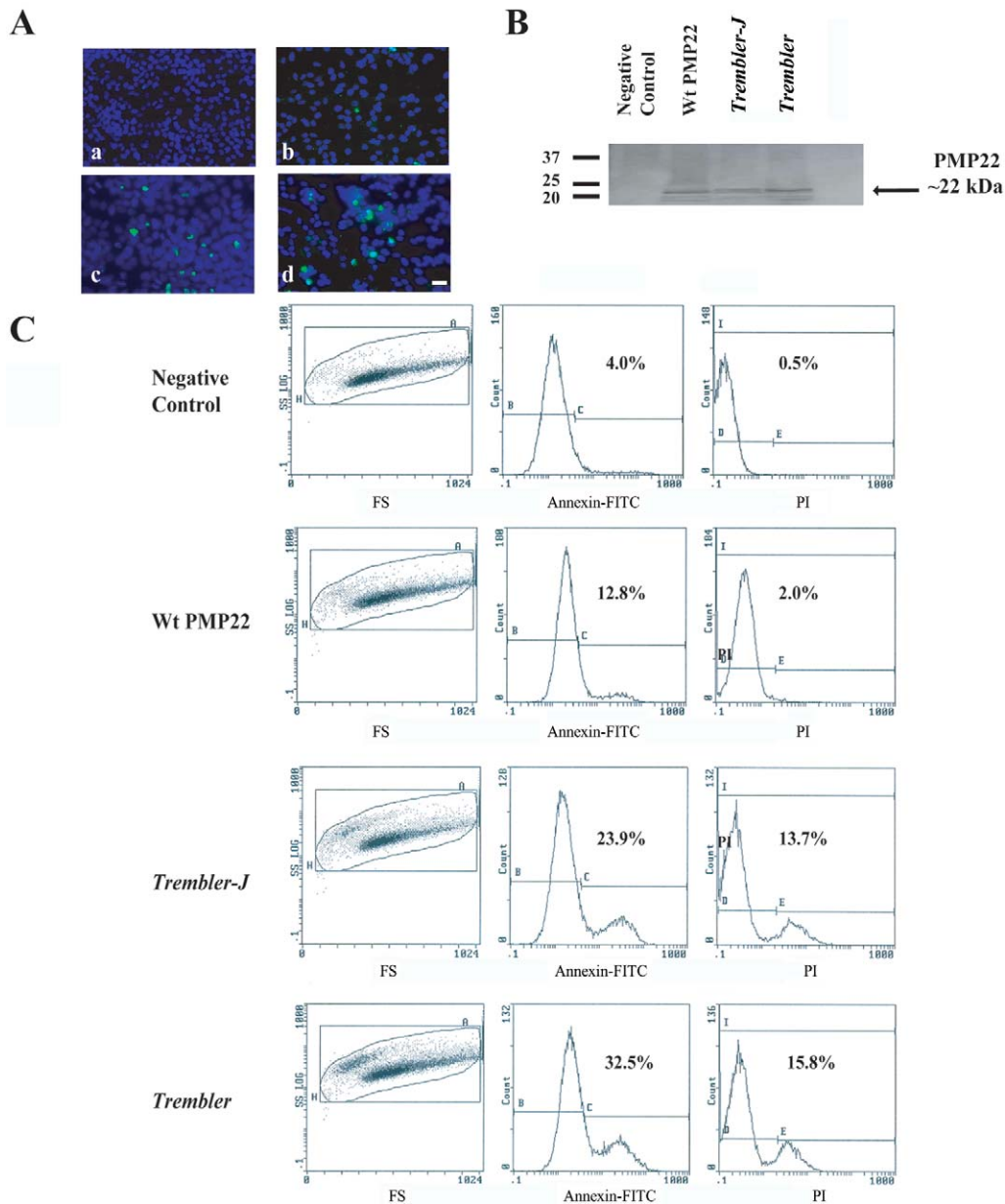
Figure 2. Increased cell death in HeLa cells after transfection with *Tr-J* and *Tr* mutations. *A,* Apoptosis induced in HeLa cell lines after transient transfection (scale bar = 25 μm). Cell lines transfected with wild-type (Wt) *PMP22* (*b*) show a significantly lower number of positive cells. Data from TUNEL assays revealed the presence of more TUNEL-positive cells only after transfection with *Tr-J* (*c*) and *Tr* (*d*) mutations. Negative control cells (*a*) transfected with empty plasmid are also shown. *B,* Western-blot analysis showing similar PMP22 protein levels (*arrow*) for both wild-type and mutants in transiently transfected HeLa cell lines. Quantitative RT-PCR experiments revealed equal amounts of mRNA in the experimental and control samples, which is consistent with the western blots (not shown). *C,* Representative study of the flow-cytometric analysis of apoptosis after transfection of cells with wild-type *PMP22*, *Tr-J,* and *Tr*. Significant differences were observed in the percentage of cells undergoing apoptosis when transfected with *Tr-J* and *Tr,* showing a higher toxic effect of those mutations on cells compared with that of wild-type *PMP22* (representative data are from one of four independent experiments with comparable results). FS = flow-sorted cells; PI = propidium iodide.

Schwann cells.[24,25,30] Both overexpression of wild-type PMP22 and mutant Tr-J protein form a complex with calnexin, a Ca^{2+}-binding chaperone, that contributes to ER retention.[30] To independently verify these earlier findings in our experimental paradigm, we transiently transfected wild-type *PMP22* cDNA and *Tr-J* and *Tr* mutations in HeLa cells. HeLa cells transfected with wild-type *PMP22* expressed the PMP22 protein on the plasma membrane, and both Tr-J and Tr mutants were detectable within the cell and were not incorporated into plasma membrane (fig.

1*A*). Accumulation of mutant PMP22 in the ER could be potentially accounted for by its interaction with calnexin and perhaps the triggering of the unfolded protein response; however, markers of the unfolded protein response are not significantly changed in heterozygous *Tr-J* sciatic nerves.[30,31] Alternatively, aggregation of Tr-J and Tr mutants in the ER and formation of a complex with calnexin may instead compromise the ability of calnexin to retain GD3 synthase (ST8), a key component for ceramide-induced apoptosis,[32] thus sensitizing the cells to apoptosis.

To determine whether the death of cells expressing *Tr-J* and *Tr* mutants are apoptotic, we performed TUNEL labeling on cells transfected with wild-type and *PMP22* mutants. We quantified the number of positive cells by counting all TUNEL-positive cells and DAPI-positive nuclei in 10 sections of the chamber slides. We found a large number of positive cells among those transfected with *Tr-J* and *Tr* compared with cells expressing wild-type *PMP22* ($P = .00014$ and $P = .0089$, respectively) (fig. 2*A*). To exclude the possibility that the apoptosis may represent a nonspecific consequence of protein overexpression, we performed a western analysis. We found similar PMP22 protein levels for both wild type and mutants in transiently transfected HeLa cell lines (fig. 2*B*). We also documented equal amounts of *PMP22* mRNA in the experimental and control samples by quantitative RT-PCR experiments, consistent with the western analysis (data not shown).

As an independent experimental approach, we also used a combined annexin V–propidium iodide assay to quantify cell apoptosis of transiently transfected HeLa cells with *Tr-J* and *Tr* mutations. Our analyses confirmed that *Tr-J* and *Tr* mutations induce apoptosis, with the annexin V–positive cells reaching percentages of 25.9% and 32.5%, respectively (fig. 2*C*). Interestingly, cells transfected with wild-type *PMP22* contained a relatively higher percentage of apoptotic cells (13.1%) than did the negative control transfected with empty plasmid (4%) (fig. 2*C*). This may result from overexpression of wild-type PMP22 that can accumulate to a level in ER that is toxic to cells.

We showed recently that ER-retained MPZ-truncating mutants, associated with severe forms of peripheral neuropathy, are released into the cytoplasm after curcumin supplementation, apparently enabling more-efficient protein processing. Such improved processing is accompanied by reduced apoptosis.[29] To assess whether curcumin treatment is sufficient to mitigate the toxic effect of PMP22-mutant aggregation in cells, we measured cell apoptosis after treatment with curcumin in HeLa cells transiently transfected with PMP22 mutants for 24 h (fig. 3). Notably, we observed a decrease in apoptosis, possibly after more-efficient protein processing, by treating the cells with 40 μM of curcumin (figs. 1*B* and 3). The percentage of apoptotic cells after treatment (12.3% and 15.9% for *Tr-J* and *Tr,* respectively) is reduced from that observed without

curcumin treatment and is similar to that observed for the wild-type PMP22 (fig. 3).

Improved Motor Performances with Curcumin Treatment

The above studies document that curcumin can mitigate the toxicity of neuropathy-causing PMP22 mutant proteins in cell culture, as we demonstrated elsewhere for disease-associated MPZ mutants.[29] We then sought to evaluate the potential therapeutic use of oral curcumin supplementation in vivo by use of the *Tr-J* mouse model. We treated 20 newborn *Tr-J* mice (13 female and 7 male) with daily doses of curcumin (50 and 100 mg per kg of body weight) by force feeding orally for 90 d. We also administered the placebo (containing alimentum only) to 6 female and 5 male mice. Curcumin dosing was based on previous studies and on what is apparently tolerated in humans, calculated on the basis of dosage weight per body weight.[33] After treatment, we measured the motor performances of each animal by the standard rotarod test. This allowed us to compare the motor coordination and balance of the treated and untreated groups of mice.

In a series of 10 consecutive trials, the duration that the animals remained on the stepwise-accelerating rotating rod was measured and plotted (fig. 4*A*). We observed a significant difference ($P < .0001$) in motor performance between treated (with 50 or 100 mg/kg curcumin) and untreated *Tr-J* mice (fig. 4*A*). *Tr-J* mice were able to remain on the rotarod for a shorter period of time (average 7 s) than were wild-type and treated *Tr-J* mice (average 270 s and 155 s, respectively). Treatment at the higher dose of 100 mg/kg showed a greater improvement in motor performance (fig. 4*A*); thus, we continued the higher dose. Although the average walking time spent on the rod for treated *Tr-J* mice was less than the time for the wild-type mice, mice of both sexes treated with curcumin performed significantly better than did the placebo and untreated *Tr-J* mice ($P < .0001$) (fig. 4*A*). Curcumin treatment did not affect the growth of the animals, as evidenced by serial weight measurements, and had no apparent toxic effect at the doses tested in our study, as revealed by comparison of treated and untreated wild-type animals (data not shown).

To determine whether this improvement in *Tr-J* motor performance was a direct result of curcumin treatment, we performed a second series of trials, using identical conditions to the first trial, except that curcumin supplementation was discontinued after 3 mo of treatment. As in the first trial, we confirmed the initial improvement of motor performance in the standard rotarod test after curcumin treatment (fig. 4*B*). We did not observe a significant difference in motor performance of *Tr-J* mice within 1 mo after discontinuation of treatment (trials 12–22; fig. 4*B*); however, 2 mo after treatment was ceased (trials 23–26), *Tr-J* mice started to weaken significantly compared with those that were treated continuously ($P < .001$) (fig. 4*B*). Our data indicate a dose-dependent significant improve-

ment of motor coordination and muscle strength in *Tr-J* mice treated with oral curcumin supplementation that is reversed after curcumin withdrawal.

We also treated a limited number of adult *Tr-J* animals (data not shown) but discontinued the treatment because we observed no significant improvement in phenotype. We noted that a greater improvement in phenotype was seen when newborn *Tr-J* mice were treated than when treatment was initiated in adulthood.

Decreased in Vivo Cell Death of Schwann Cells with Curcumin Treatment

Experiments in vivo have suggested a significant increase in apoptotic Schwann cells in sciatic nerves of 3-wk-old

Tr mice that continues to be prominent in adult mutant mice, compared with wild-type mice.[34] We measured the frequency of Schwann cell apoptosis in sciatic nerves of *Tr-J* mice. We observed a considerable number of apoptotic cells in *Tr-J* mice, whereas there was only minor or no detectable cell death in the sciatic nerves from wild-type animals (fig. 5A). As observed in earlier studies of *Tr* mice,[34] we also detected a significant increase in Schwann cell density in nerves from our *Tr-J* animals, despite the increased rate of cell loss, possibly reflecting the unmasking of axon-derived Schwann cell mitogens, such as glial growth factor (or heregulin). To evaluate whether curcumin may have similar effects on Schwann cells as those seen in cell culture assays (i.e., reducing the cytotoxicity
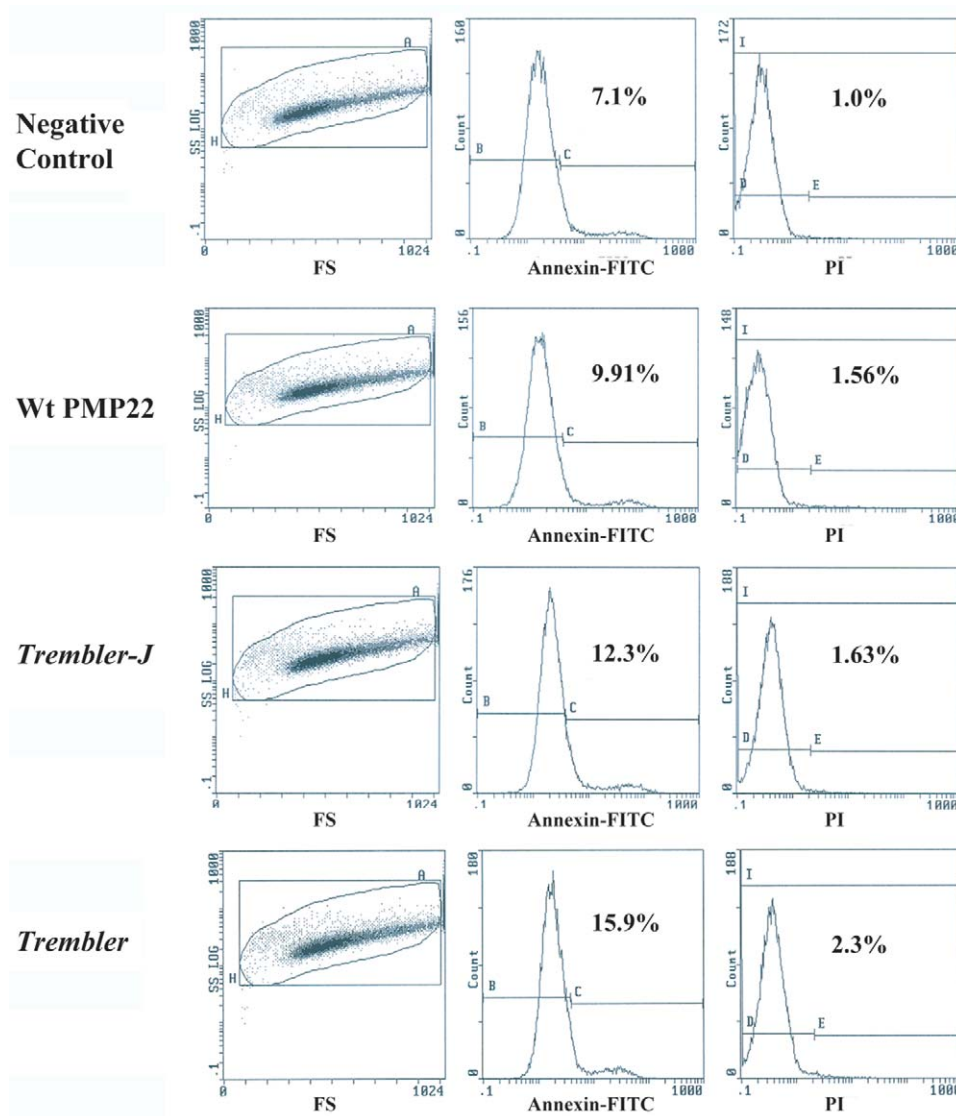

Figure 3. Curcumin's reversal of induction of apoptosis. Shown are results of apoptosis analysis of cells transiently transfected with wild-type (Wt) *PMP22, Tr-J,* and *Tr* mutations after curcumin treatment. Note that the percentage of apoptotic cells after curcumin treatment is significantly different from that observed for no treatment (fig. 2) (representative data are from one of four independent experiments with comparable results). FS = flow-sorted cells; PI = propidium iodide.
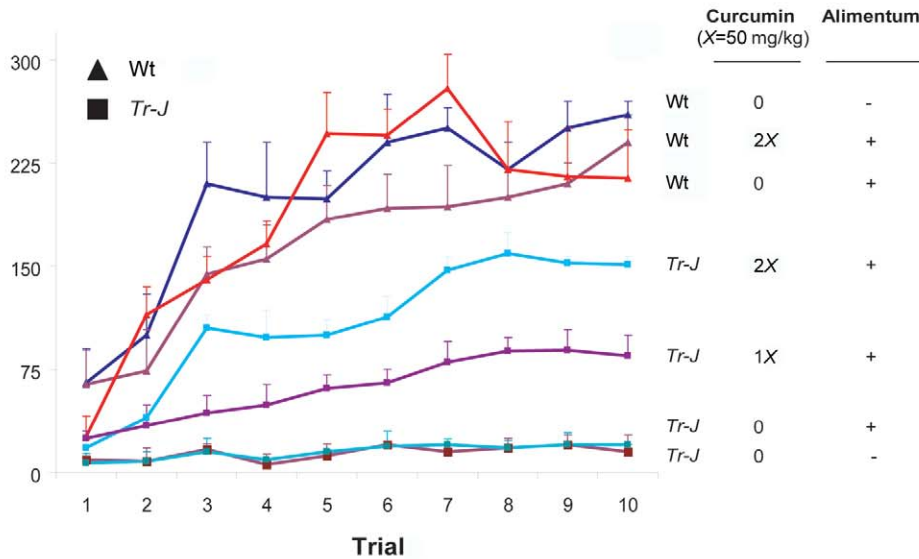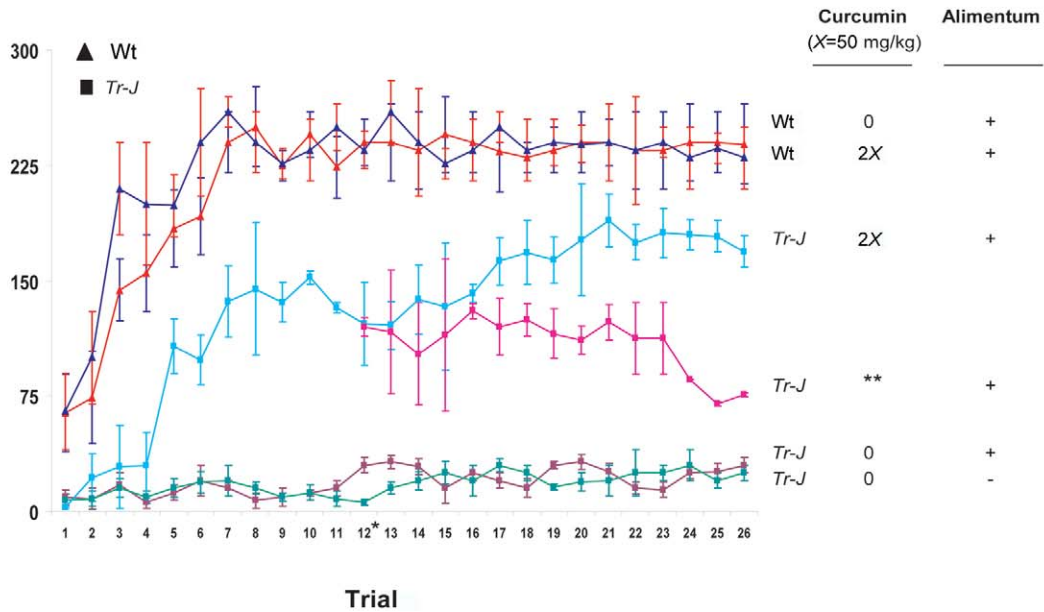
Figure 4. Improved neuromotor behavior in treated *Tr-J* mice. *A,* Rotarod test performed with 3-mo-old wild-type (Wt), *Tr-J,* curcumin-treated *Tr-J,* and placebo-treated mice. In three series and 10 trials, the time that animals remained on a rod was measured and plotted. The rotation speed was increased every minute, from 16 to 36 rpm, in steps of 4 rpm. The mean holding time of curcumin-treated *Tr-J* mice (*n* = 20) was significantly higher than that of placebo and *Tr-J* mice (*n* = 10). All animals were allowed to stay on the rod for a maximum of 270 s. *B,* Curcumin treatment was discontinued for a group of *Tr-J* mice (*n* = 5) after 3 mo of treatment. The rotarod test was performed similar to as described above, after curcumin treatment followed by discontinuation of treatment (marked on the *X*-axis with an asterisk [*]). We did not observe significant difference in the motor performance of *Tr-J* mice at 1 wk (trials 12–14), 2 wk (trials 15–18), and 1 mo (trials 19–22) after withdrawal of curcumin. *Tr-J* mice started to weaken significantly at 2 mo after treatment was ceased (trials 23–26) (*P* < .001). A double asterisk (**) denotes the group of mice (*n* = 5) that were originally treated with curcumin for 3 mo and then had the treatment discontinued.
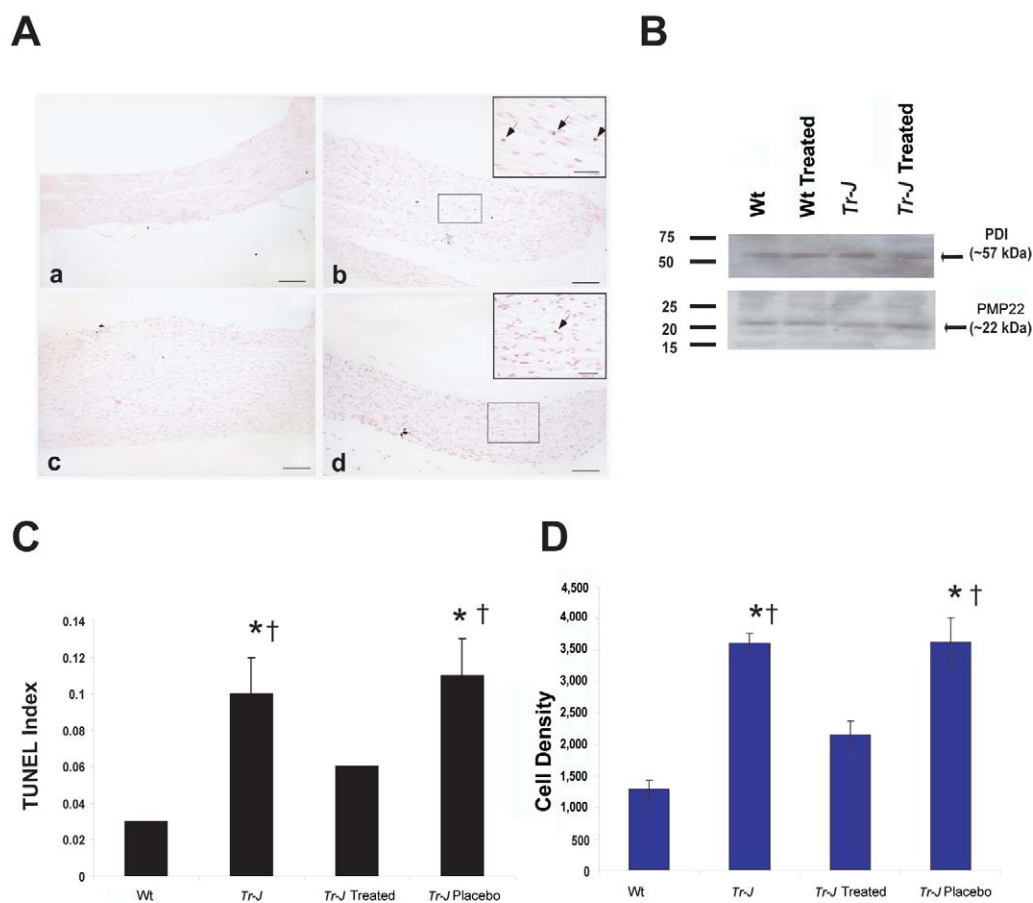
A

B

C

D

Figure 5. In vivo TUNEL staining of longitudinal sections of *Tr-J* and treated *Tr-J* sciatic nerves. *A,* Longitudinal sections of sciated nerve of wild-type (*a*), *Tr-J* (*b*), curcumin-treated *Tr-J* (*c*), and placebo-treated *Tr-J* (*d*) mice. The scale bar is 40 μm for the inset and 100 μm for the lower-power resolution. Arrows indicate TUNEL-positive cells. *B,* Western-blot analysis showing similar PMP22 protein levels for both wild-type (Wt) and *Tr-J* mice before and after curcumin treatment. *C,* Quantification of apoptosis in the sciatic nerves of wild-type, curcumin-treated, and placebo-treated *Tr-J* mutants. *D,* Quantitative analysis of cell density per mm² in wild-type control, *Tr-J*, placebo-treated *Tr-J,* and curcumin-treated *Tr-J* sciatic nerves. An asterisk (*) and a dagger (†) denote statistically significant differences from the wild-type and curcumin-treated *Tr-J* mice, respectively. Note that there is no statistically significant difference between the *Tr-J* mice and the *Tr-J* mice treated with placebo.

of mutant proteins and lowering the percentage of apoptotic cells [fig. 3]), we examined, in a blinded fashion, the cell death of Schwann cells in sciatic nerves of curcumin-treated *Tr-J* mice and compared it with that in placebo-treated *Tr-J* and wild-type control mice.

We observed significantly reduced Schwann cell apoptosis ($P < .001$) in curcumin-treated *Tr-J* mice compared with in placebo-treated *Tr-J* animals (fig. 5*A* and 5*C*). Although there is no evidence that curcumin may increase or decrease the expression of *Pmp22,* western analysis of curcumin-treated and placebo-treated *Tr-J* mice show equal amounts of PMP22 protein before and after treatment (fig. 5*B*). This suggests that curcumin treatment conceivably relieves the toxic effect of mutant PMP22 in *Tr-J* mice and inhibits Schwann cell apoptosis, the in vivo correlate to our cell culture assay. Notably, this results in improvement of the clinical and neuropathologic phenotype of the *Tr-J* mice.

To confirm the presence of curcumin in adult treated *Tr-J* mice, we measured the level of curcumin in different tissues at 0, 0.5, and 2 h after oral administration. We found a considerable amount of curcumin in liver (1,086.3 ng/ml in adult and 403 ng/ml in pup) within 0.5 h after treatment, which declined after 2 h (table 1). However, curcumin levels peaked at 2 h in blood (1,079.27 ng/ml), brain (330.14 ng/ml), and sciatic nerves (453.8 ng/ml) (table 1). In a standard control, curcumin was detected and analyzed by HPLC with UV absorption at a range of 190–800 nm and by ion-selected monitoring in mass spectrometry (fig. 6*A* and 6*B*). Curcumin detected in all tissue samples of treated mice had the same retention time as the curcumin standard (fig. 7). We were also able to measure the concentration of curcumin present in tissues after 30 min and up to 2 h after treatment (table 1).

A previous study[35] found very low levels of curcumin present in serum after oral administration, raising ques-

Table 1. Curcumin Bioavailability Study in Mice

Sample	Tissue Amount	Curcumin (ng)	Curcumin Concentration (ng/ml)
Adult mouse:			
Liver (0 h)	.19 g	UD	UD
Liver (.5 h)	.23 g	249.85	1,086.30
Liver (2 h)	.21 g	98.59	469.50
Blood (0 h)	.23 ml	UD	UD
Blood (.5 h)	.40 ml	150.83	377.08
Blood (2 h)	.35 ml	377.74	1079.27
Brain (0 h)	.16 g	UD	UD
Brain (.5 h)	.19 g	UD	UD
Brain (2 h)	.15 g	49.52	330.14
Sciatic nerve (0 h)[a]	.028 g	UD	UD
Sciatic nerve (.5 h)[a]	.03 g	UD	UD
Sciatic nerve (2 h)[a]	.034 g	15.43	453.82
2-wk-old pup:			
Liver (0 h)	.17 g	UD	UD
Liver (.5 h)	.08 g	32.26	403.36
Liver (2 h)	.13 g	32.51	250.07
Blood (0 h)	.12 ml	UD	UD
Blood (.5 h)	.15 ml	UD	UD
Blood (2 h)	.1 ml	33.46	334.61
Brain (0 h)	.34 g	UD	UD
Brain (.5 h)	.26 g	UD	UD
Brain (2 h)	.20 g	37.28	186.41
Sciatic nerve (0 h)[b]	.018 g	UD	UD
Sciatic nerve (.5 h)[b]	.024 g	15.20	633.33
Sciatic nerve (2 h)[b]	.0225 g	15.18	674.67

NOTE.—UD = undetectable.

[a] Curcumin was not detectable in sciatic nerves by UV/VIS detector. We used a pool of two adult mice samples, and curcumin was detected by fluorescence detectors.

[b] Curcumin was not detectable in sciatic nerves by UV/VIS detector. We used a pool of three pup samples, and curcumin was detected by fluorescence detectors.

tions about the bioavailability of the compound to tissues and target cells. We have also found that the levels of curcumin in serum are very low, virtually undetectable by use of our methods (data not shown). This result is not surprising, because curcumin is a very hydrophobic compound and would be expected to partition into cellular membranes. Our analysis of whole blood and tissues confirms that this is the case and that orally administered curcumin does indeed make its way into tissues throughout the body, including the brain and peripheral nerves. We used a fluorescence detector to determine the amount of curcumin in sciatic nerve, because of the low volume of nerve tissue. The total amount of curcumin detected was lower than in other tissues, despite its high concentration in nerve (fig. 6C). The concentration of curcumin in sciatic nerve of treated *Tr-J* mice is apparently sufficient to reduce the cytotoxicity of mutant PMP22 in the mice (fig. 5C). Interestingly, curcumin concentrations in sciatic nerves of treated 2-wk-old *Tr-J* pups were higher than those in treated adult *Tr-J* mice (table 1). A combination of higher curcumin bioavailability and more-active myelination in *Tr-J* pups may account for the greater improvement observed in the phenotype of newborn treated *Tr-J* mice than *Tr-J* mice treated during adulthood.

We also compared the cell density in sciatic nerves of curcumin-treated *Tr-J* mice with that in wild-type and placebo-treated *Tr-J* mice. Interestingly, we detected a decrease in Schwann cell density in sciatic nerves of treated *Tr-J* mice (fig. 5D), suggesting a possible reduction of cell proliferation as a result of either more successful myelination or less demyelination of axons by Schwann cells in the treated *Tr-J* animals. These data imply that premature apoptotic death of Schwann cells due to ER retention of mutant PMP22 may be a pathomechanism responsible for the inability of *Tr-J* mice to form normal myelin and that treatment with curcumin reduces the cytotoxicity of mutant proteins by lowering the percentage of apoptotic Schwann cells (fig. 5C).

Improved Axonal Size and Decrease in Neurofilament (NF) Density with Curcumin Treatment

To understand better the basis for the clinical and neuropathologic improvement in animals associated with oral curcumin supplementation, we performed a morphological analysis of sciatic nerves of curcumin-treated and placebo-treated *Tr-J* mice (fig. 8A). We measured both the axonal and fiber diameters of ~2,000 myelinated axons (table 2) from three curcumin-treated *Tr-J* mice, three placebo-treated *Tr-J* mice, and two wild-type mice. Placebo-treated *Tr-J* mice showed histological hallmarks of CMT1, as observed previously in *Tr-J* mice,[17] whereas curcumin-treated *Tr-J* mice had a higher average fiber and axonal size (fig. 8B and 8C and table 2). In addition, curcumin-treated *Tr-J* mice had significantly ($P = 10^{-16}$) increased myelin thickness (g ratio [$\pm$SD] of 0.74 ± 0.07; $n = 3$) compared with that of placebo-treated *Tr-J* mice (g ratio of 0.81 ± 0.07; $n = 3$) (fig. 8D and table 2). Thus, the combination of increased axonal caliber and myelin thickness may explain the phenotypic improvement in curcumin-treated *Tr-J* mice.

We also analyzed the NF densities by electron microscopy in cross-sections through axons of sciatic nerves from placebo-treated *Tr-J,* curcumin-treated *Tr-J,* and wild-type control mice (fig. 9). NFs were spaced randomly throughout cross-sections of all samples, which allowed an accurate calculation of NF densities. We did not characterize NF densities in nodal and paranodal regions because those regions have increased NF densities compared with those of normal axons.[36] We selected axons with similar diameters from each animal, and the observer was blinded to genotype and treatment status. There were 195 ± 32.75 NFs per μm^2 in control (wild-type) mice, 265 ± 37.75 NFs per μm^2 in curcumin-treated *Tr-J* mice, and 485 ± 41.15 NFs per μm^2 in placebo-treated *Tr-J* mice axons. This represents a significant difference between curcumin-treated and placebo-treated animals ($P < .0001$). Such a decrease in NF density suggests increased spacing between NFs that is correlated with higher NF phosphorylation and is directly modulated by axon–Schwann cell interactions during myelination.[37] This observation agrees well with our earlier findings by light microscopy of increased axonal
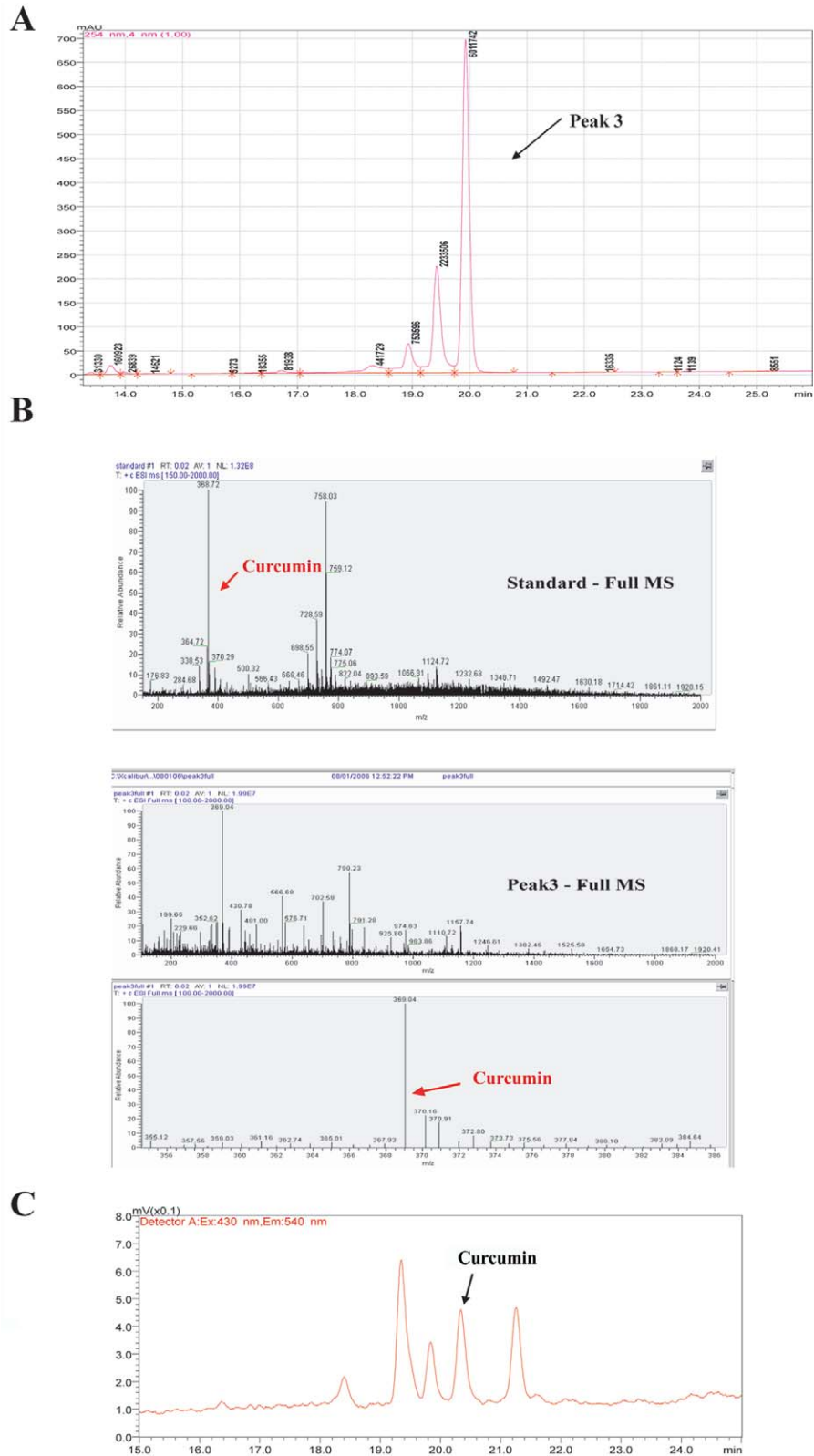
Figure 6. HPLC and mass-spectrometry analyses of curcumin. *A,* Curcumin detected with UV/VIS (190–800 nm) or fluorescence (excitation at 430 nm; emission at 540 nm) detectors. *B,* Verification of the peak corresponding to curcumin by mass spectrometry (MS) analysis. *C,* HPLC analysis of sciatic nerves after curcumin treatment. Because of the low levels of curcumin in sciatic nerves, curcumin was not detectable by UV/VIS; instead, fluorescence detectors were used. The curcumin peak (*arrow*) in the sciatic nerves had the same retention time as in the curcumin standard. No peak was observed at this position in samples from mice that did not receive curcumin treatment.
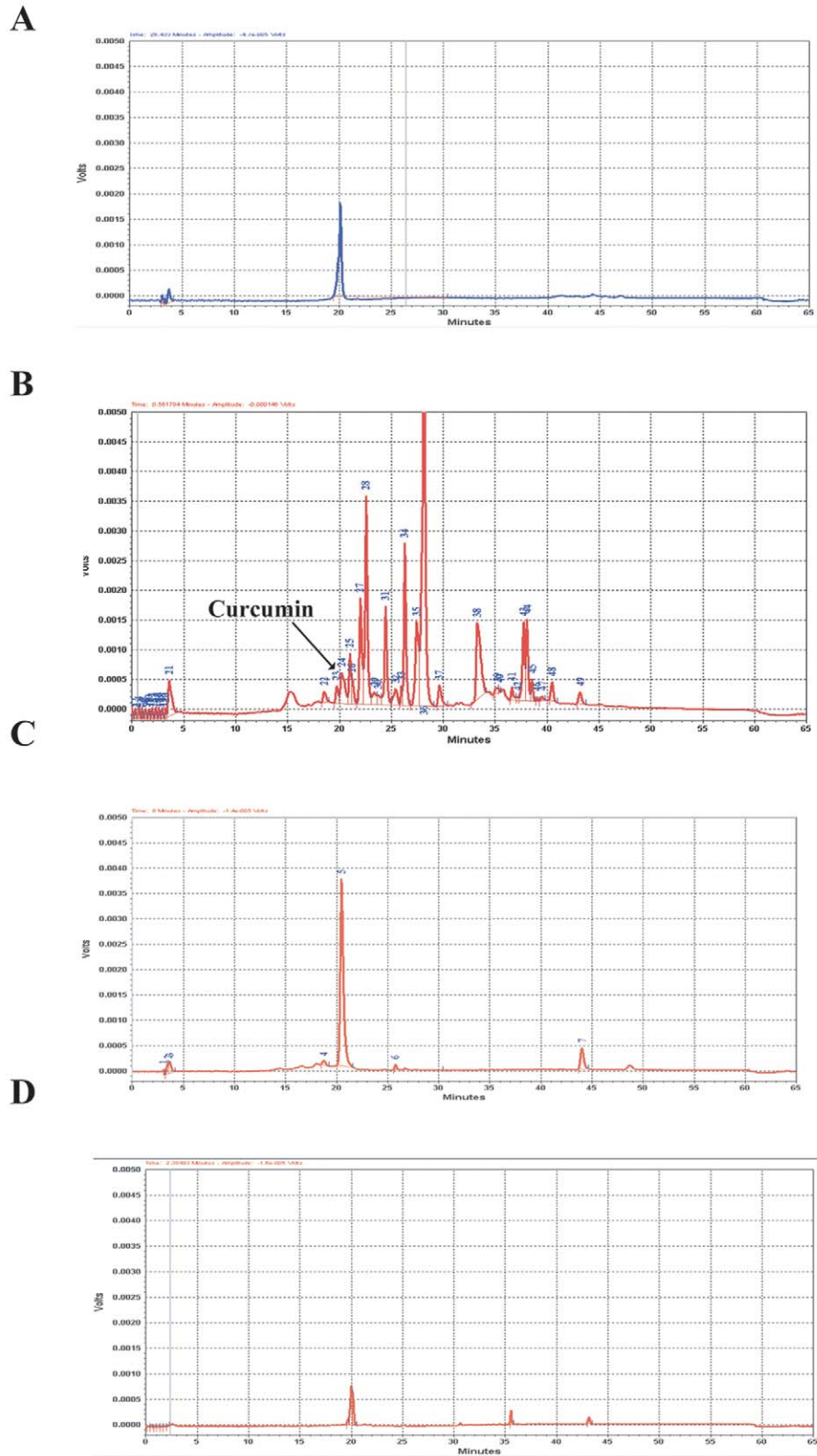
Figure 7. Curcumin bioavailability assayed by HPLC analysis in multiple tissues after curcumin treatment. Curcumin has a retention time of 20 min in the standard (*A*). Curcumin was detected in liver (*B*), blood (*C*), and brain (*D*) of 2-wk-old pups after curcumin treatment. We also detected curcumin in treated adult mice in a similar pattern.
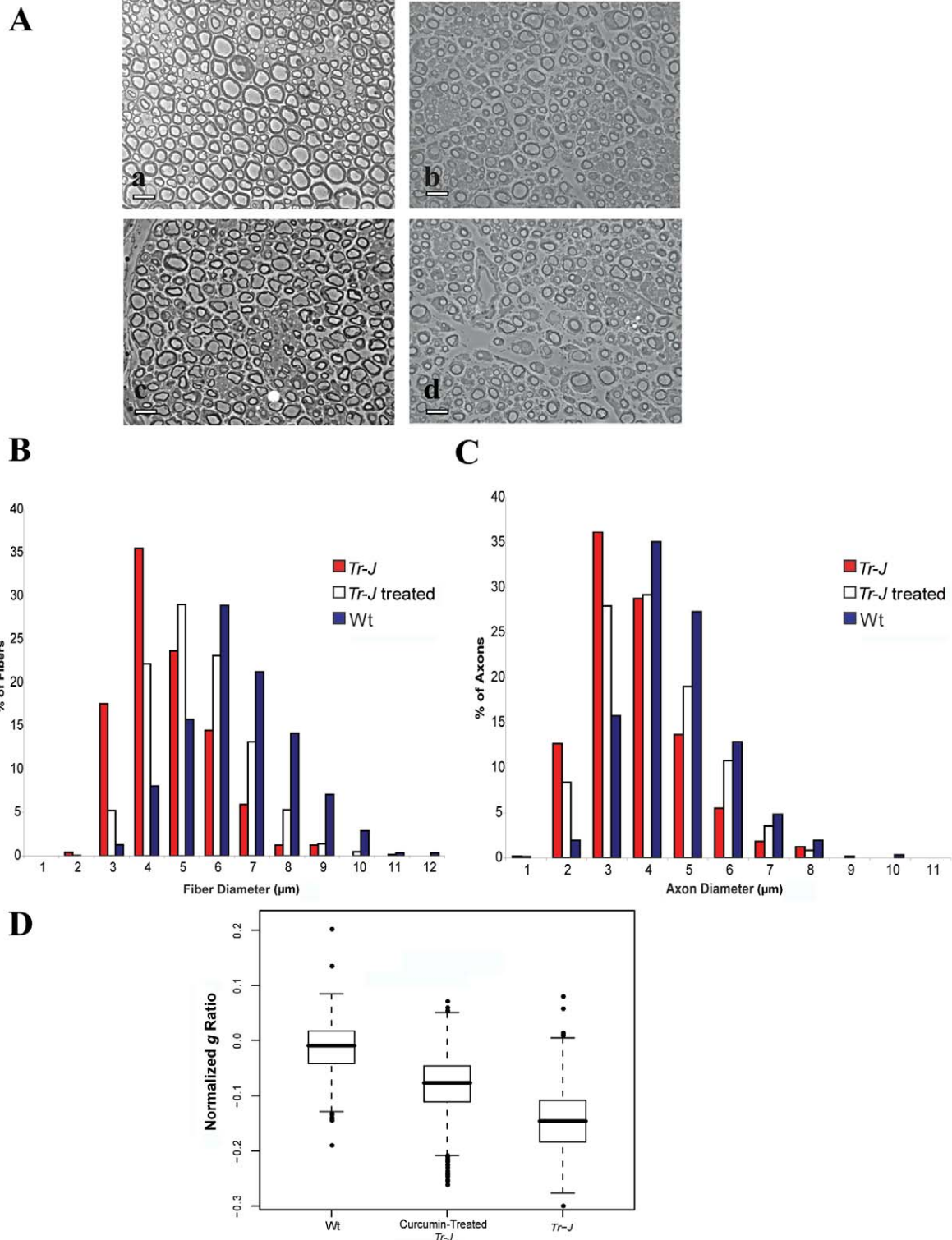
448

Figure 8. Histopathology and quantitative analyses of normal, *Tr-J,* and treated *Tr-J* sciatic nerves. *A,* Note the difference in morphology and mean axonal diameter of myelinated fibers in wild-type normal (*a*), *Tr-J* (*b*), curcumin-treated *Tr-J* (*c*), and placebo-treated *Tr-J* (*d*) sciatic nerves from 3-mo-old mice. Scale bars = 10 μm. *B,* Distribution of fiber size (based on diameter) in *Tr-J* (*red*), curcumin-treated *Tr-J* (*white*), and wild-type control (*blue*) mice. *C,* Distribution of axonal size in *Tr-J* (*red*), curcumin-treated *Tr-J* (*white*), and wild-type control (*blue*) mice. *D,* Normalized plot of *g* ratios within each group, to account for the trends (nonlinear) between axon size and the ratio observed in the wild-type mice.

449

Table 2. Comparison of the Morphological Characteristics of Wild-Type, *Tr-J*, and Treated *Tr-J* Sciatic Nerve

Characteristic	Wild Type	*Tr-J*	Treated *Tr-J*	*Tr-J* with Alimentum Only
Mean axonal diameter of myelinated fibers (μm)	4.82 $\pm$ 1.2	3.73 $\pm$ 1.21	4.10 $\pm$ 1.29	3.75 $\pm$ 1.16
Mean fiber diameter (μm)	6.88 $\pm$ 1.4	4.63 $\pm$ 1.23	5.41 $\pm$ 1.34	4.61 $\pm$ 1.20
g ratio	.69 $\pm$ .05	.80 $\pm$ .06	.74 $\pm$ .07	.81 $\pm$ .07

size and more myelinated axons in sciatic nerves of treated *Tr-J* mice.

Discussion

We investigated the biological effect of curcumin in Schwann cells of *Tr-J* mice and evaluated its potential therapeutic use for selected forms of inherited peripheral neuropathies that result from protein misfolding or aggregation in the ER. We found that oral administration of curcumin to newborn *Tr-J* mice significantly improves, in a dose-dependent manner, the motor coordination and muscle strength of living mice by apparently relieving the toxic effect of Tr-J and Tr aggregation–induced apoptosis or generalized cell stress. The presence of curcumin in blood and sciatic nerves (table 1) within 2 h after treatment in both pups and adults demonstrates its bioavailability for mitigating the toxic effect of PMP22 mutant aggregation in Schwann cells, as observed in our cell culture assays. We also found that, even though the thickness of the myelin sheath was reduced in curcumin-treated mice in comparison with that in wild-type mice, it was nevertheless sufficient to improve the motor performance of *Tr-J* mice as measured by the rotarod test.

We also analyzed the possibility that the pathological improvements may be the result of curcumin's action through the NF-κB pathway. NF-κB inhibition is known to reduce macrophages, and an increased number of macrophages has been observed in sciatic nerves of animal models for CMT1A,[38] suggesting that macrophages may play an active role in myelin degeneration. Given this observation, we performed a macrophage-specific F4/80 stain on sciatic nerves of wild-type, untreated *Tr-J*, placebo *Tr-J*, and curcumin-treated *Tr-J* mice and observed no significant change in macrophages between our tested groups of mice (data not shown). In aggregate, these data suggest that curcumin relieves the toxicity and/or cell stress associated with the *Tr-J* mutation and enables a more efficient protein-trafficking process in the ER that can result in increased axonal size and myelination that is sufficient to improve the clinical phenotype of *Tr-J* mice.

Many diseases are linked to the accumulation of proteins in the ER, suggesting that misfolding often occurs in that cellular compartment.[39] Protein misfolding can contribute to disease through different mechanisms. Disease etiology may result when the efficiency of productive folding and/or trafficking is reduced to a threshold point at which there is not enough properly trafficked, functional protein to maintain normal physiological function (i.e., a loss-of-function disease mechanism). An alternative is a gain-of-function disease mechanism, in which the aberrant protein actively promotes pathogenesis due to changes of normal protein function[40] or formation of toxic aggregates, such as amyloid.[28]

We evaluated the use of curcumin for treatment of severe forms of CMT that are caused by mutant proteins with a gain of function and with a more deleterious effect because of being misprocessed in the cell.[41] Our data document the reduction in the percentage of apoptotic cells for mutants in cell culture. In vivo studies confirmed the findings of our cell culture assays and showed reduced apoptosis in biopsies of sciatic nerves from curcumin-treated *Tr-J* mice. The point at which PMP22 in *Tr-J* exerts its apparent cytotoxic effects has not been determined, but putative "gain-of-function" effects of PMP22 with the *Tr-J* mutation include sequestration of ER chaperones, such as calnexin; the formation of aggregates (presumably in the ER); or inhibition of post-ER (cytoplasmic) protein-degradation pathways. However, histological analyses of curcumin-treated *Tr-J* mice nerves (figs. 5 and 8) display a morphologic phenotype that is less severe than that which results from a gain-of-function *Tr-J* mutation. Curcumin treatment could potentially lessen ER accumulation and improve trafficking of Schwann cell proteins in general or PMP22 in particular, resulting in improved myelination of Schwann cells, a decrease in NF densities, and an increased axonal caliber.

Our data could be important not only for patients with inherited peripheral neuropathies but also for patients with other diseases caused by aberrant proteins that promote disease etiology by the formation of toxic aggregates. Curcumin treatment of animal models also provides a better understanding of the pathological disease mechanisms caused by ER-retained mutants, such as the majority of rhodopsin mutants that have been linked to phenotypes of retinitis pigmentosa[42] or mutant proteolipid proteins that cause Pelizaeus-Merzbacher disease (PMD), a CNS dysmyelinating disorder.[43] A misfolded protein can accumulate to a level in which ER-associated degradation (ERAD) gets overwhelmed, resulting in oversaturation of the components of ERAD. For example, the myelin proteolipid protein (PLP) is produced in vast quantities by myelinating oligodendrocytes.[44] Abnormal amounts of disrupted proteolipid proteins in the ER can overwhelm both ERAD and

A

B

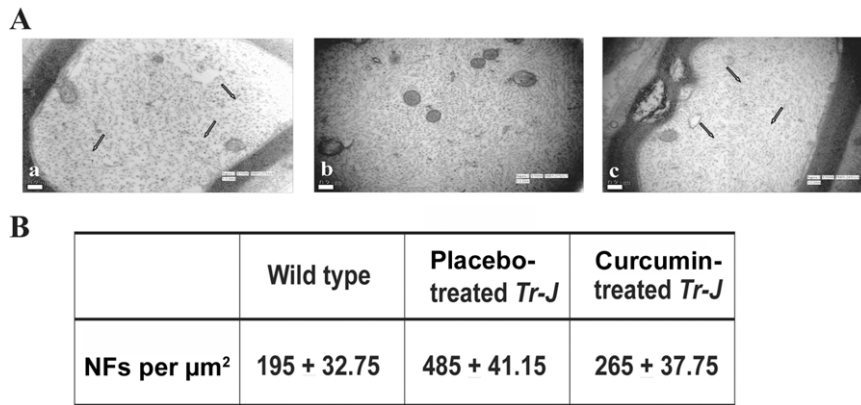|	Wild type	Placebo-treated *Tr-J*	Curcumin-treated *Tr-J*
NFs per µm²	195 + 32.75	485 + 41.15	265 + 37.75

Figure 9. *A,* Electron micrographs of normal, *Tr-J,* and treated *Tr-J* sciatic nerves. In wild-type control mice (*a*), NFs are relatively sparse (*arrows*), whereas, in *Tr-J* mice (*b*), the NFs are increased in number. In curcumin-treated *Tr-J* mice (*c*), NFs (*arrows*) become less compact compared with those in untreated *Tr-J* mice (*b*). Scale bars = 0.2 μm. *B,* Calculation of the average number of NF per axonal diameter in wild-type control, *Tr-J,* and curcumin-treated *Tr-J* mice. NFs are increased significantly (*P* < .001) in number in *Tr-J* mice compared with in curcumin-treated *Tr-J* mice and wild-type mice.

normal export pathways, potentially provoking the unfolded-protein response and major changes in cell physiology that result in oligodendrocyte apoptosis in PMD animal models.[45]

In such cases, rational drug design could be based on different principles, such as interfering with chaperone activity, enabling misfolded proteins to traverse out of the ER, or potentially modulating protein folding.[46] Analysis of curcumin bioavailability (table 1) has also shown the presence of curcumin in brain within 2 h after treatment (with 100 mg of curcumin per kg of body weight) in both pups and adults tested in our study, suggesting that it might cross the blood-brain barrier and reach the brain in treated mice. Thus, curcumin could be a promising new therapeutic agent and may prove useful for disorders such as PMD, since it appears to be stable and present in brain with no apparent toxic effects. However, further investigation to determine the direct effects of curcumin on PLP mutants in cell culture is necessary. Curcumin can apparently rescue misfolded proteins by potentially interfering with the function of ER calcium-dependent chaperones.[26] However, curcumin modulates a number of cellular messenger pathways, including NF-κB and intracellular calcium,[26,47] that have been associated with the regulation of myelination.

In summary, there are a number of cellular mechanisms by which curcumin could have acted on *Tr-J* nerves. First, curcumin protects Schwann cells from apoptosis that is induced by the presence of the PMP22 mutant protein. The ability of curcumin to increase axonal caliber and myelin thickness, without tomaculae formation, is consistent with the hypothesis that curcumin relieves ERAD stress caused by abnormal processing of PMP22 and/or other Schwann cell proteins that are required for myelination. Finally, it is formally possible that curcumin might modulate signal-transduction pathways that regulate my-

elin gene expression. Alternatively, curcumin may act directly on neurons by acting on signal-transduction pathways, to mimic the trophic effect of myelinating Schwann cells on axonal caliber. Although these latter two hypotheses may serve to explain the clinical effects of curcumin on the *Tr-J* neuropathy, they do not explain the reduced rate of apoptosis observed in curcumin-treated *Tr-J* sciatic nerves.

In conclusion, we have shown that curcumin treatment partially mitigates the clinical and neuropathologic phenotype of *Tr-J* mice by relieving the toxic effect of the mutant PMP22, thereby inhibiting Schwann cell apoptosis and increasing axonal caliber and myelin thickness. Furthermore, this positive clinical response to curcumin occurs in a dose-dependent manner and is reversed after withdrawal of treatment. Notably, there were no side effects observed in treated mice at each of the doses tested in our study. Further studies are recommended with other mouse models, such as *Tr, Tr-m1H,* or *Tr-m2H*[19], that represent more-severe human peripheral neuropathy, as well as with *Pmp22*-overexpressing mice, to evaluate the potential use of curcumin for therapy of more selected forms of inherited peripheral neuropathies. Such studies will likely provide further insights into common pathomechanisms and enable a better understanding of the pathophysiology of these disorders.

Web Resources

The URLs for data presented herein are as follows:

Inherited Peripheral Neuropathies Mutation Database, http://www.molgen.ua.ac.be/CMTMutations/

Online Mendelian Inheritance in Man (OMIM), http://www.ncbi.nlm.nih.gov/Omim/ (for CMT1, CMT2, HNPP, DSN, and CHN)

References

1. Skre H (1974) Genetic and clinical aspects of Charcot-Marie-Tooth's disease. Clin Genet 6:98

2. Lupski JR, Garcia CA (2001) Charcoat-Marie-Tooth peripheral neuropathies and related disorders. In: Scriver CR, Beaudet AL, Sly WS, Valle D (eds) The metabolic and molecular basis of inherited diseases. McGraw-Hill, New York, pp 5759–5788

3. Shy ME, Lupski JR, Chance PF, Klein CJ, Dyck PJ (2005) Hereditary motor and sensory neuropathies: an overview of clinical, genetic, electrophysiologic, and pathologic features. In: Dyck PJ, Thomas PK (eds) Peripheral neuropathy. Elsevier Saunders, Philadelphia, pp 1623–1658

4. Timmerman V, Lupski JR, De Jonghe P (2006) Molecular genetics, biology, and therapy for inherited peripheral neuropathies. Neuromolecular medicine special issue. Humana Press, Totowa, NJ, pp 1–278

5. Lupski JR, de Oca-Luna RM, Slaugenhaupt S, Pentao L, Guzzetta V, Trask BJ, Saucedo-Cardenas O, Barker DF, Killian JM, Garcia CA, et al (1991) DNA duplication associated with Charcot-Marie-Tooth disease type 1A. Cell 66:219–232

6. Raeymaekers P, Timmerman V, Nelis E, De Jonghe P, Hoogendijk JE, Baas F, Barker DF, Martin JJ, De Visser M, Bolhuis PA, et al (1991) Duplication in chromosome 17p11.2 in Charcot-Marie-Tooth neuropathy type 1a (CMT 1a). The HMSN Collaborative Research Group. Neuromuscul Disord 1:93–97

7. Lupski JR, Wise CA, Kuwano A, Pentao L, Parke JT, Glaze DG, Ledbetter DH, Greenberg F, Patel PI (1992) Gene dosage is a mechanism for Charcot-Marie-Tooth disease type 1A. Nat Genet 1:29–33

8. Chance PF, Alderson MK, Leppig KA, Lensch MW, Matsunami N, Smith B, Swanson PD, Odelberg SJ, Disteche CM, Bird TD (1993) DNA deletion associated with hereditary neuropathy with liability to pressure palsies. Cell 72:143–151

9. Chance PF, Abbas N, Lensch MW, Pentao L, Roa BB, Patel PI, Lupski JR (1994) Two autosomal dominant neuropathies result from reciprocal DNA duplication/deletion of a region on chromosome 17. Hum Mol Genet 3:223–228

10. Lupski JR, Chance PF (2005) Hereditary motor and sensory neuropathies involving altered dosage or mutation of *PMP22*: the CMT1A duplication and HNPP deletion. In: Dyck PJ, Thomas PK (eds) Peripheral neuropathy. Elsevier Saunders, Philadelphia, pp 1659–1680

11. Pareek S, Suter U, Snipes GJ, Welcher AA, Shooter EM, Murphy RA (1993) Detection and processing of peripheral myelin protein PMP22 in cultured Schwann cells. J Biol Chem 268: 10372–10379

12. Snipes GJ, Suter U, Welcher AA, Shooter EM (1992) Characterization of a novel peripheral nervous system myelin protein (PMP-22/SR13). J Cell Biol 117:225–238

13. Haney C, Snipes GJ, Shooter EM, Suter U, Garcia C, Griffin JW, Trapp BD (1996) Ultrastructural distribution of PMP22 in Charcot-Marie-Tooth disease type 1A. J Neuropathol Exp Neurol 55:290–299

14. Martini R (1997) Animal models for inherited peripheral neuropathies. J Anat 191:321–336

15. Sereda MW, Meyer zu Horste G, Suter U, Uzma N, Nave KA (2003) Therapeutic administration of progesterone antagonist in a model of Charcot-Marie-Tooth disease (CMT-1A). Nat Med 9:1533–1537

16. Passage E, Norreel JC, Noack-Fraissignes P, Sanguedolce V, Pizant J, Thirion X, Robaglia-Schlupp A, Pellissier JF, Fontes M (2004) Ascorbic acid treatment corrects the phenotype of a mouse model of Charcot-Marie-Tooth disease. Nat Med 10: 396–401

17. Suter U, Moskow JJ, Welcher AA, Snipes GJ, Kosaras B, Sidman RL, Buchberg AM, Shooter EM (1992) A leucine-to-proline mutation in the putative first transmembrane domain of the 22-kDa peripheral myelin protein in the *Trembler-J* mouse. Proc Natl Acad Sci USA 89:4382–4386

18. Suter U, Welcher AA, Ozcelik T, Snipes GJ, Kosaras B, Francke U, Billings-Gagliardi S, Sidman RL, Shooter EM (1992) Trembler mouse carries a point mutation in a myelin gene. Nature 356:241–244

19. Isaacs AM, Davies KE, Hunter AJ, Nolan PM, Vizor L, Peters J, Gale DG, Kelsell DP, Latham ID, Chase JM, et al (2000) Identification of two new Pmp22 mouse mutants using large-scale mutagenesis and a novel rapid mapping strategy. Hum Mol Genet 9:1865–1871

20. Valentijn LJ, Baas F, Wolterman RA, Hoogendijk JE, van den Bosch NH, Zorn I, Gabreels-Festen AW, de Visser M, Bolhuis PA (1992) Identical point mutations of PMP-22 in *Trembler-J* mouse and Charcot-Marie-Tooth disease type 1A. Nat Genet 2:288–291

21. Ionasescu VV, Searby CC, Ionasescu R, Chatkupt S, Patel N, Koenigsberger R (1997) Dejerine-Sottas neuropathy in mother and son with same point mutation of *PMP22* gene. Muscle Nerve 20:97–99

22. Notterpek L, Shooter EM, Snipes GJ (1997) Upregulation of the endosomal-lysosomal pathway in the trembler-J neuropathy. J Neurosci 17:4190–4200

23. Naef R, Suter U (1999) Impaired intracellular trafficking is a common disease mechanism of PMP22 point mutations in peripheral neuropathies. Neurobiol Dis 6:1–14

24. Colby J, Nicholson R, Dickson KM, Orfali W, Naef R, Suter U, Snipes GJ (2000) PMP22 carrying the Trembler or Trembler-J mutation is intracellularly retained in myelinating Schwann cells. Neurobiol Dis 7:561–573

25. Fortun J, Go JC, Amici SA, Dunn WA Jr, Notterpek J (2006) Alterations in degradative pathways and protein aggregation in a neuropathy model based on *PMP22* overexpression. Neurobiol Dis 22:153–164

26. Egan ME, Pearson M, Weiner SA, Rajendran V, Rubin D, Glockner-Pagel J, Canny S, Du K, Lukacs GL, Caplan MJ (2004) Curcumin, a major constituent of turmeric, corrects cystic fibrosis defects. Science 304:600–602

27. Teijido O, Martinez A, Pusch M, Zorzano A, Soriano E, Del Rio JA, Palacin M, Estevez R (2004) Localization and functional analyses of the MLC1 protein involved in megalencephalic leukoencephalopathy with subcortical cysts. Hum Mol Genet 13:2581–2594

28. Yang F, Lim GP, Begum AN, Ubeda OJ, Simmons MR, Am-

begaokar SS, Chen PP, Kayed R, Glabe CG, Frautschy SA, et al (2005) Curcumin inhibits formation of amyloid beta oligomers and fibrils, binds plaques, and reduces amyloid *in vivo*. J Biol Chem 280:5892–5901

29. Khajavi M, Inoue K, Wiszniewski W, Ohyama T, Snipes GJ, Lupski JR (2005) Curcumin treatment abrogates endoplasmic reticulum retention and aggregation-induced apoptosis associated with neuropathy-causing myelin protein zero-truncating mutants. Am J Hum Genet 77:841–850

30. Dickson KM, Bergeron JJ, Shames I, Colby J, Nguyen DT, Chevet E, Thomas DY, Snipes GJ (2002) Association of calnexin with mutant peripheral myelin protein-22 *ex vivo*: a basis for "gain-of-function" ER diseases. Proc Natl Acad Sci USA 99:9852–9857

31. Kamholz J, Awatramani R, Menichella D, Jiang H, Xu W, Shy M (1999) Regulation of myelin-specific gene expression: relevance to CMT1. Ann N Y Acad Sci 883:91–108

32. Tomassini B, Malisan F, Franchi L, Nicolo C, Calvo GB, Saito T, Testi R (2004) Calnexin suppresses GD3 synthase-induced apoptosis. FASEB J 18:1553–1555

33. Cheng AL, Hsu CH, Lin JK, Hsu MM, Ho YF, Shen TS, Ko JY, Lin JT, Lin BR, Ming-Shiang W, et al (2001) Phase I clinical trial of curcumin, a chemopreventive agent, in patients with high-risk or pre-malignant lesions. Anticancer Res 21:2895–2900

34. Sancho S, Young P, Suter U (2001) Regulation of Schwann cell proliferation and apoptosis in PMP22-deficient mice and mouse models of Charcot-Marie-Tooth disease type 1A. Brain 124:2177–2187

35. Song Y, Sonawane ND, Salinas D, Qian L, Pedemonte N, Pedemonte N, Galietta LJ, Verkman AS (2004) Evidence against the rescue of defective ΔF508-CFTR cellular processing by curcumin in cell culture and mouse models. J Biol Chem 279:40629–40633

36. Price RL, Paggi P, Lasek RJ, Katz MJ (1988) Neurofilaments are spaced randomly in the radial dimension of axons. J Neurocytol 17:55–62

37. Starr R, Attema B, DeVries GH, Monteiro MJ (1996) Neurofilament phosphorylation is modulated by myelination. J Neurosci Res 44:328–337

38. Kobsar I, Hasenpusch-Theil K, Wessig C, Muller HW, Martini R (2005) Evidence for macrophage-mediated myelin disruption in an animal model for Charcot-Marie-Tooth neuropathy type 1A. J Neurosci Res 81:857–864

39. Muchowski PJ, Wacker JL (2005) Modulation of neurodegeneration by molecular chaperones. Nat Rev Neurosci 6:11–22

40. Lester HA, Karschin A (2000) Gain of function mutants: ion channels and G protein-coupled receptors. Annu Rev Neurosci 23:89–125

41. Snipes GJ, Orfali W, Fraser A, Dickson K, Colby J (1999) The anatomy and cell biology of peripheral myelin protein-22. Ann N Y Acad Sci 883:143–151

42. Garriga P, Manyosa J (2002) The eye photoreceptor protein rhodopsin: structural implications for retinal disease. FEBS Lett 528:17–22

43. Inoue K (2005) PLP1-related inherited dysmyelinating disorders: Pelizaeus-Merzbacher disease and spastic paraplegia type 2. Neurogenetics 6:1–16

44. Bronstein JM (2000) Function of tetraspan proteins in the myelin sheath. Curr Opin Neurobiol 10:552–557

45. Gow A, Southwood CM, Lazzarini RA (1998) Disrupted proteolipid protein trafficking results in oligodendrocyte apoptosis in an animal model of Pelizaeus-Merzbacher disease. J Cell Biol 140:925–934

46. Yang PW, Kumar TK, Jayaraman G, Yu C (1996) Effect of organic acids in the prevention of aggregation on rapid refolding of proteins. Biochem Mol Biol Int 38:393–399

47. Sarkar FH, Li Y (2004) Cell signaling pathways altered by natural chemopreventive agents. Mutat Res 555:53–64